Available online at www.eccomasproceedia.org
Eccomas Proceedia SMART (2023) 1657-1668

ECCOMAS
Proceedia

X ECCOMAS Thematic Conference on Smart Structures and Materials
SMART 2023
D.A. Saravanos, A. Benjeddou, N. Chrysochoidis and T. Theodosiou (Eds)

STACKED MULTI-LAYER CAPACITIVE STRAIN SENSOR BASED ON DIELECTRIC ELASTOMERS

Artem Prokopchuk[1], Arthur Ewert[2], Johannes D. M. Menning[3], Andreas Richter[1], Berthold Schlecht[2], Thomas Wallmersperger[3] and E.-F. Markus Henke[1,4]

[1]Institute for Semiconductors and Microsystems, Technische Universität Dresden, Nöthnitzer Straße 64, 01069 Dresden
e-mail: artem.prokopchuk1@tu-dresden.de

[2] Institute of Machine Elements and Machine Design, Technische Universität Dresden, Münchner Platz 3, 01069 Dresden

[3] Institute of Solid Mechanics, Technische Universität Dresden, George-Bähr-Str. 3c, 01069 Dresden

[4] PowerON Group, 1010 Auckland, New Zealand

Abstract. In recent years, conventional machine elements have begun to gain new capabilities due to the sensor-integration processes. Couplings are one such central machine element in mechanical engineering. To make couplings "smart" machine elements, it is necessary to equip them with a sensor. Due to the high deformation requirements of embedded sensors, a dielectric elastomer sensor (DES) concept was chosen, and implemented in the deforming elastic gear rim of the jaw coupling. In this work we present the manufacturing and stacking of a multi-layer capacitive strain sensors in the form of an electric multi-layer circular capacitor (ML-DES). The design of DES is represented by an elastomeric substrate with alternating layers of conductive silicone-based ink as the circular capacitor plates and an elastomeric film as the dielectric and electrical insulation. A variety of thin ML-DES with four electrode layers were fabricated to evaluate the stacking process (4ML-DES). The manufactured sensors were tested using tensile testing machine and an LCR meter. It can be shown that the viscoelasticity of the dielectric elastomer material affects the behavior of the change in capacitance. Comparing different stacked and unstacked sensors, it has been determined that the capacitance change of stacked sensor is more stable. The design of the sensor was adapted to the elastic element of the jaw coupling. For the stacked sensor consisting of three 4ML-DES was determined a Gauge Factor (GF) of $GF_{3x4ML-DES} = 1.59$.

Key words: Capacitive strain sensor, Multi-layer dielectric elastomer sensor, Carbon black based electrodes, Jaw coupling, Sensor-integrating machine elements

Peer-review under responsibility of the organizing committee of SMART 2023.
doi: 10.7712/150123.9937.445520

1 INTRODUCTION

Researchers are currently paying significant attention to soft sensors due to their potential to enable efficient interaction between humans and intelligent systems, including applications such as electronic skins, monitoring and control systems, and the Internet of Things (IoT). Traditional rigid sensors are typically used in industry to monitor and control the state of a machine system [1]. Machines typically consist of many elements that move, rotate, hold, transmit torque, etc. One of these machine elements that transmit rotational motion or torque from one shaft to another are couplings, in particular elastic couplings. There are various types of sensors that are used in automation, to monitor various parameters of a machine element: temperature sensors, pressure sensors, level sensors, strain sensors [2, 3], infrared sensors, proximity sensors, optical sensors, MEMS sensors, etc. Strain sensors are commonly used to measure the deformation experienced by objects [4]. There are various types of strain sensors, each designed for specific applications and requirements. Ma et al. [5] reviewed different transition mechanisms of flexible strain sensors. Some common types of strain sensors include: resistive [6], capacitive [7, 8, 9, 10], piezoelectric, triboelectric, inductance/magnetic [5] and optical strain sensors [11]. Capacitive strain sensors based on dielectric elastomers are a type of soft material-based strain sensors that measure the applied strain by detecting the change in capacitance between two flexible electrodes, coated on the surface of a dielectric elastomer [12]. Dielectric elastomers are soft, rubber-like materials that exhibit large deformation under an applied electric field. The electrodes on the surface of elastomers are made of compliant conductive materials, such as carbon black conductive ink, carbon nanotubes, or silver ink. When a strain is applied to the sensor, the distance between the electrodes changes, resulting in a change in the capacitance of the system. This change in capacitance is then used to measure the applied strain. Capacitive strain sensors based on dielectric elastomers have shown great potential for various applications due to their high flexibility, sensitivity to small strains, and compatibility with soft materials.

Conceptually, the various types of capacitive strain sensors differ in terms of the adopted dielectric and electrode material, and the type of strain they can measure. The parallel plate capacitor design is mainly used for tension and compression. In addition, the capacitive strain sensor can detect bending and twisting movements and their magnitude [8, 9, 10]. Table 1 summarizes some relevant work in the field of capacitive strain sensors. Cai et al. [7] used the Dragon skin 30 elastomer and the transparent carbon nanotubes (CNT) film to achieve high sensitivity and stability of the stretch sensor. Chhetry et al. [8] fabricated a capacitive pressure sensor in the form of a dielectric hybrid polyurethane (PU) sponge consisting of calcium copper titanate ($CaCu_3Ti_4O_{12}$, CCTO). They used CCTO to increase the dielectric constant of the PU sponge, resulting in an increase in sensor capacitance. Mo and coworkers [9] utilized an organogel and a conductive hydrogel to achieve superior plastic deformability and dynamically stretchability of the sensor. Hu et al. [10] fabricated a capacitive strain sensor with a wrinkled structure to achieve high linearity and low hysteresis over a large stretch range from 0% to 300% strain. The aforementioned sensors are relatively large compared to the size of the space available in jaw coupling teeth. In this work we present a stacked structure of a compact

Table 1: Overview of existing works on capacitive strain sensors.

	Year	DE-Material	Electrode Material	Size, [mm]	Strain type	Strain value
[7]	2013	Sylgard 184/ Dragon skin 30	CNT film	rectangular 10x2x1	stretch	300%
[8]	2020	CCTO/PU	CNT/PDMS	rectangular 20x20x2	bend, twist compress	90°, 90° 76.2%
[9]	2021	PVA/PAA-borax organogel	Zn-alginate/ PAM hydrogel	circular ⌀60x3.5	stretch, bend compress	200, 150° 100%
[10]	2022	VHB tape	CNT/ Tegaderm film	rectangular 17.5x7.5x1	bend stretch	90° 300%
This work	2023	Elastosil/ SilGel 612	CB/Ecoflex-20	circular ⌀3x0.75	compress	30%

capacitive strain ML-DES. The proposed stacked sensor possesses good compressibility, due to the highly stretchable Elastosil film and carbon black (CB)/Ecoflex-20 based conductive ink used, as well as a compact size, which allows it to be further integrated into the jaw coupling.

2 CAPACITIVE MULTI-LAYER STRAIN SENSOR CONCEPT

The multi-layer DES (ML-DES) has a structure of a variable circular plate capacitors in parallel connection [13]. In this work, we investigated ML-DES with four electrode layers (4ML-DES). However, ML-DES structure with more layers will be investigated in future works. For creating the ML-DES with four electrodes, five layers of silicone elastomeric film and four electrode layers are considered. The first base elastomeric layer is a silicone substrate, the Elastosil base in Figure 1. Each following dielectric layer consists of silicone adhesive and elastomeric film, glue SilGel and Elastosil in Figure 1 respectively. An electrode pattern is alternately applied to each elastomeric film. Note that each next electrode layer is a mirror image of the previous one, and also includes the pins for implementing the electrical connections, cf. Figure 1 (top). We used a conductive ink based on Ecoflex-20 and carbon black KETJEN BLACK EC-600 JD to create the electrode layers. For simplicity, a circular electrode geometry is chosen for the active film area. Chen et al. noted that the mathematically optimized complex shape of the electrode could potentially offer even higher strains, compared to regular ones [14]. The influence of the shape of electrodes on the resulting capacity will be investigated in future works.

In this work, we present three structures: one with four electrode layers (1x4ML-DES), another composed of two 4ML-DES stacked together (2x4ML-DES), and a third consisting of three 4ML-DES stacked together (3x4ML-DES). One 4ML-DES has three capacitors C_1, C_2 and C_3 connected in parallel, cf. Figure 1 (left). The 2x4ML-DES structure has six capacitors

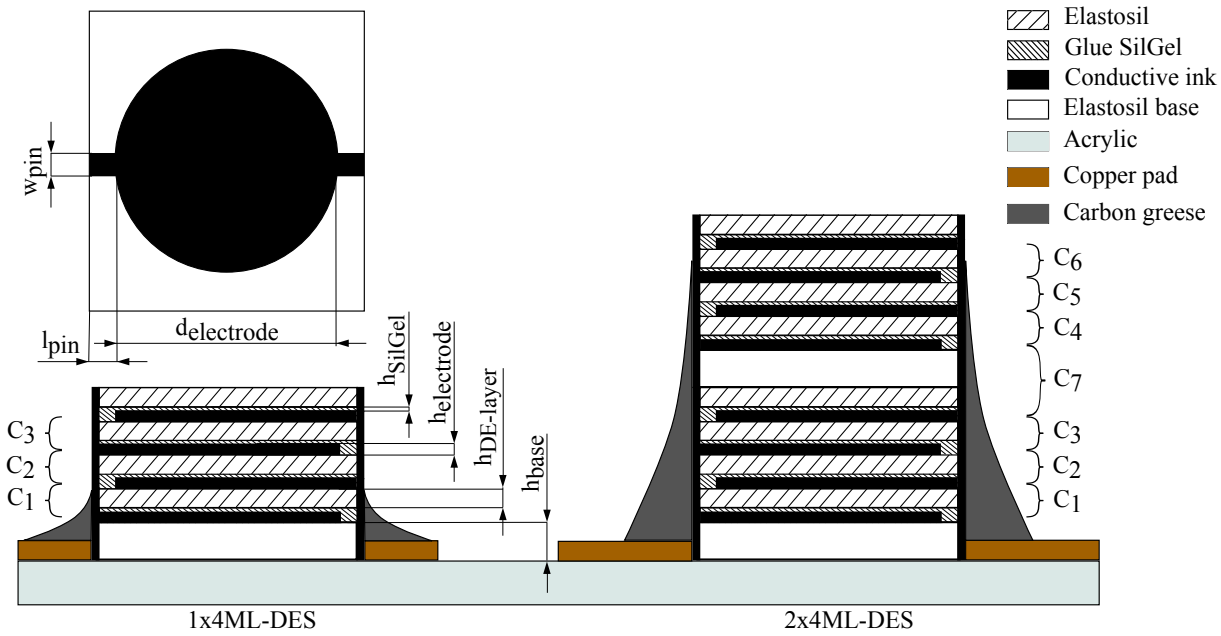

Figure 1: Multi-layer DES concept. (left) 1x4ML-DES: structure of one capacitive multi-layer sensor with four electrode layers and three capacitors C_1, C_2, C_3 connected in parallel, where $h_{\text{base}} = 100\,\mu\text{m}$ - a thickness of the Elastosil base film, $h_{\text{SilGel}} = 5\,\mu\text{m}$ - a thickness of the SilGel adhesive, $h_{\text{electrode}} = 17.5\,\mu\text{m}$, $h_{\text{DE-layer}} = 50\,\mu\text{m}$ - a thickness of the Elastosil dielectric layer; (top) top view of 1x4ML-DES: design of the electrodes with a diameter of $d_{\text{electrode}} = 3\,\text{mm}$, with a pin's length of $l_{\text{pin}} = 1.5\,\text{mm}$ and a width of $w_{\text{pin}} = 0.5\,\text{mm}$; (right) 2x4ML-DES: two 4ML-DES stacked on top of each other, eight electrode layers, six capacitors $C_1 \ldots C_6$ and one additional capacitor C_7.

$C_1 \ldots C_6$, cf. Figure 1 (right). One of the additional capacitor C_7 appears between two sensors after their combination. The dielectric layer of the capacitor C_7 consists of the Elastosil base layer with a thickness of h_{base}, the Elastosil dielectric layer with a thickness of $h_{\text{DE-layer}}$, and the adhesive SilGel layer with a thickness of h_{SilGel}, cf. Figure 1 (right). The 3x4ML-DES structure has already nine capacitors and two additional capacitors. We have not shown the 3x4ML-DES structure as it is similar to 2x4ML-DES but with one more sensor on top of it.

The stacking is applied in order to increase the number of layers and reduce the cumulative errors that accumulate during the manufacturing process. The manufacturing process is only partially automated, and we did most of the steps manually. The stacked concept enables the manufacturing of structures with more layers while avoiding a long manufacturing process and cumulative manufacturing errors. The more layers a sensor has, the higher its capacitance. The higher capacitance enables to detect the strain more precisely.

3 MANUFACTURING

The following section describes the manufacturing of the 4ML-DES, the newly applied stacking approach, and the materials used.

3.1 ML-DES manufacturing

The fabrication of ML-DES is described in detail in our previous work [15]. In the following, we will briefly describe the manufacturing process. The materials needed to manufacture the ML-DES are: (i) Elastosil film with a thickness of $h_{\mathrm{base}} = 100\,\mu\mathrm{m}$, and (ii) $h_{\mathrm{DE-layer}} = 50\,\mu\mathrm{m}$, (iii) SilGel 612 from Wacker, and (iv) conductive ink (CI). For the manufacture of ML-DES, we used: a laser cutter for cutting the printing masks, a doctor blade machine Automatic Film Applicator ZAA 2300 from Zehntner GmbH Testing Instruments for applying the layer of CI and SilGel adhesive, a roll laminator for laminating the electrode layer, and an oven for curing the applied layers.

The manufacturing process consists of the following steps: CI creation, an application process of electrodes, and the lamination process.

In turn, the creation of the CI consists of the following steps: weigh the Ecoflex-20 in a ratio of part A and part B 1:1 by weight; weigh 5.76 wt% of CB, add three metal balls with a diameter of $d_{\mathrm{metal\,ball}} = 8\,\mathrm{mm}$ and grind using a planetary mixer Thinky ARE-250; weigh the solvent OS-20 in a ratio 1:1.1 to Ecoflex by weight; use the planetary mixer for 3 minutes at 2000 rpm to mix all components. Thus, the carbon black based CI is obtained.

The next step is the application process of electrodes: clean the surface of the Elastosil base film; place the PET mask on the Elastosil base film; apply some CI to the PET mask just before the cutouts; adjust the blade gap so that there is no space between the blade and the PET mask; use doctor blade to apply the electrode layer to the base layer; remove the PET mask and cure the deposited electrode layer in an oven at 100°C for 10 minutes; cool the cured electrode layer at room temperature for 10 minutes.

The lamination process is used to apply the dielectric layer of the Elastosil film and is carried out as follows: mix the SilGel adhesive in a ratio of the parts A and B 1:1 by weight; take the cooled electrode layer and place it on the doctor blade machine; place a PET strips on the edges of the Elastosil base film; adjust the blade gap of $h_{\mathrm{gap}} = 75\,\mu\mathrm{m}$ between the blade and the PET mask; apply the SilGel to the PET mask and use doctor blade to apply the SilGel layer; remove the PET strips and place the Elastosil base film on the surface of the laminator; use the roll laminator to apply the Elastosil dielectric layer with a thickness of $h_{\text{DE-layer}} = 50\,\mu\mathrm{m}$ to the Elastosil base; put the laminated layer on an aluminum board and fix it with adhesive tape; cure the laminated layer in an oven at 100°C for 30 minutes and then cool it at room temperature for 30 minutes; slowly peel off the PET supporting layer from the Elastosil dielectric layer. Now the electrode layer is insulated with the SilGel adhesive layer and the Elastosil film.

In order to obtain a structure with four electrode layers, we repeated steps 2 and 3 three more times. Thus, a multi-layer capacitive structure with four electrode layers is obtained.

3.2 ML-DES stacking

To achieve higher ML-DES capacitance, we can continue to apply electrode layers and laminate them. However, manufacturing errors accumulate during the manufacturing process and wrinkles and bumps appear on the surface of the Elastosil. The ML-DES stacking process helps to reduce the number of manufacturing steps, even though the process requires additional sensor fusion. In order to measure capacitance, the sensor must have stable contacts. We used carbon grease and copper pads to create the appropriate contacts.

The stacking of two or more 4ML-DES is conducted in the following order: First, pre-cut half of the pins' length to get high-quality layers of pin electrodes [15]. Then place each sensor on top of the other, so that the electrodes lie exactly on top of each other. The insulated electrode layers were electrically connected to each other using a brush with carbon grease. Then the sensor was placed on a special acrylic tool so that both ML-DES pins were on the copper pads, cf. Figure 2 (a). The connection between the pins and the copper pads was painted with the carbon grease brush. Finally, the sensor was fixed in the acrylic tool and is ready for testing.

4 METHODS

In order to determine how the sensor behaves according to the various factors, we studied (i) the variety of strains, (ii) the variation in strain rate, (iii) the number of stacked sensors, and (iv) the resulting capacitance.

Load tests are conducted on a ZwickRoell Z005 tensile testing machine with a $5\,\mathrm{kN}$ force cell, cf. Figure 2 (b). Experiments are conducted in a displacement-controlled manner. The preload speed is set to $V_{\mathrm{preload}} = 0.05\,\mathrm{mm\,s^{-1}}$. Various maximal strains and strain rates are chosen, as will be explained in section 5. It is important to choose the maximum strain at which the deformation of the sensor is still elastic and not plastic. The preload force is set to $F_{\mathrm{preload}} = 0.02\,\mathrm{N}$. Force and displacement of the specimen are recorded in the test software TestXpert from ZwickRoell

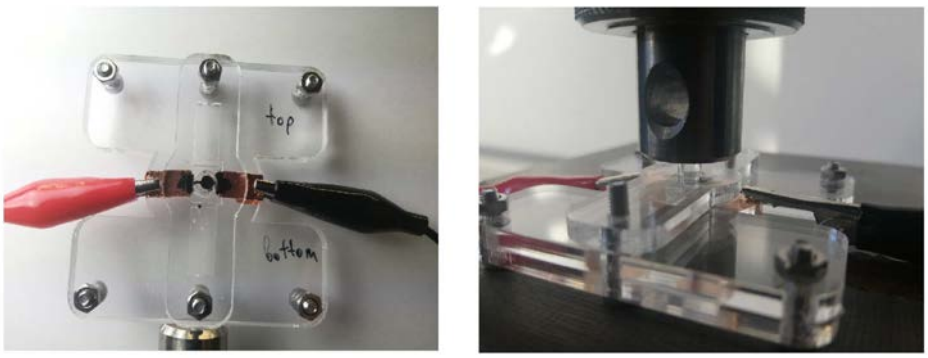

a b

Figure 2: Experimental setup. (a) The sensor is electrically connected to the copper pads, fixed in the acrylic tool, and connected to the LCR meter to measure the capacitance. (b) The sensor with the acrylic tool is placed in the tensile testing machine.

and exported in a Microsoft Excel file for further processing. The tensile testing machine has a measurement frequency of $f = 10\,\text{Hz}$.

The capacitance of the manufactured ML-DES was measured using an IM3523 LCR meter from HIOKI. The LCR meter has been set in $C_p - D$ mode, i.e. the capacitance was measured in parallel. The excitation frequency of the LCR meter was set to $f = 1\,\text{kHz}$ for all measurements.

5 RESULTS AND DISCUSSIONS

Three versions of ML-DES with one, two and three sensors have been successfully stacked and tested using an LCR meter to evaluate capacitance and a tensile test machine for applying force.

5.1 Capacitance evaluation

In order to estimate the initial capacitance of the stacked sensors used, we measured the capacitance of each 4ML-DES used for 1x4ML-DES, 2x4ML-DES and 3x4ML-DES, cf. Table 2. As can be seen from Table 2, there is a difference between the measured initial capacitance of the stacked sensors C_0 and the expected one C_{exp}. The expected capacitance is the sum of the capacitances of the individual sensors C_1, C_2, C_3. In order to evaluate this difference, we used the following formula for relative error (RE): $RE(C) = 100\% \cdot |C_{exp} - C_0| / C_0$. The difference is probably caused by losses when connecting the sensors to each other using carbon grease.

Table 2: Capacitance of the sensors used for stacking (C_1, C_2, C_3), expected (C_{exp}) and measured initial capacitance of stacked sensors (C_0), and the relative error ($RE(C)$).

	C_1, pF	C_2, pF	C_3, pF	C_{exp}, pF	C_0, pF	$RE(C)$, %
1x4ML-DES	9.88	-	-	9.88	9.88	-
2x4ML-DES	10.63	10.39	-	21.02	20.92	0.5
3x4ML-DES	10.21	10.05	10.01	30.27	30.91	2.1

For the stacked sensors tested, the change in capacitance has a similar behavior in each compression cyclic test: (i) there is a decrease in the upper threshold of capacitance change; (ii) an increase in the lower threshold of capacitance change; (iii) the capacitance change range increases with increasing strain rate, cf. Figures 3, 4, 5 (d-f); (iv) sensor relaxation - the sensor returns to its original state after the end of the cyclic test, and (v) an upward shift of the lower threshold of capacitance change with increasing strain value, cf. Figures 3, 4, 5 (a-c).

The results of cyclic compression tests on the 1x4ML-DES are shown in Figure 3. For the constant strain rate of $\dot{\lambda} = 0.01\,\text{s}^{-1}$, $0.1\,\text{s}^{-1}$ and $1\,\text{s}^{-1}$, as the strain value increases, the lower threshold of the capacitance change increases and the upper threshold decreases, cf. Figure 3 (a-c). This trend is more noticeable at higher strain rates, cf. Figures 3 (b, c). At the same time, the upward shift in the lower capacitance threshold is observed, which is also associated with

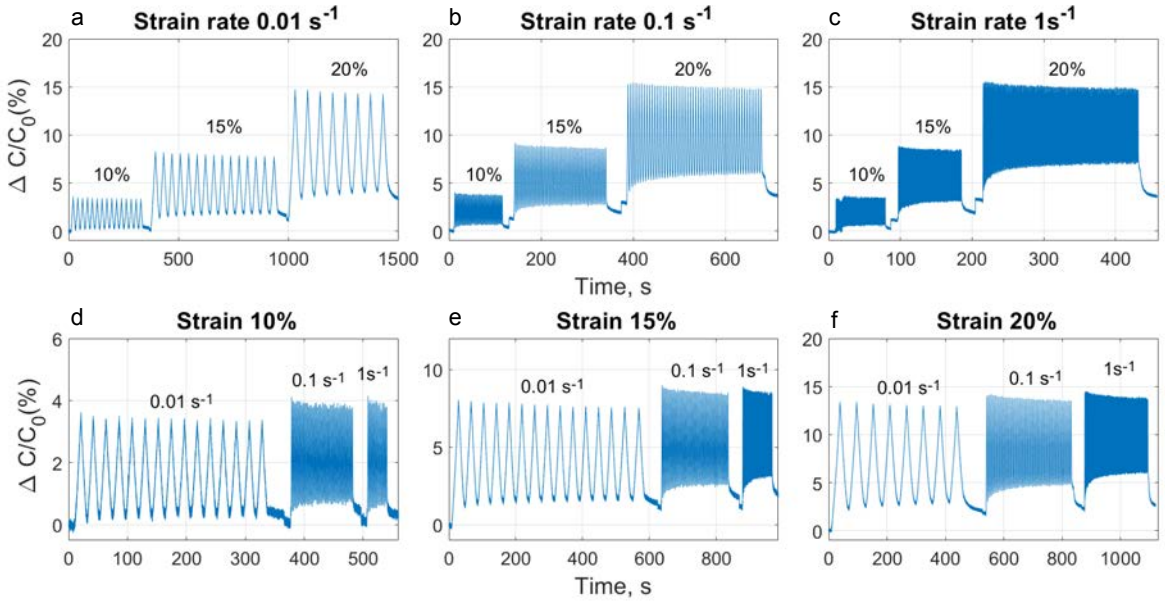

Figure 3: Cyclic compression tests on the 1x4ML-DES. (a-c) Relative changes in capacitance for various maximum strain of 10%, 15% and 20%: (a) at a constant strain rate of $\dot{\lambda} = 0.01\,\mathrm{s}^{-1}$ for 15, 15 and 8 cycles respectively; (b) at a constant strain rate of $\dot{\lambda} = 0.1\,\mathrm{s}^{-1}$ with 50 cycles each; (c) at a constant strain rate of $\dot{\lambda} = 1\,\mathrm{s}^{-1}$ for 100, 100 and 200 cycles respectively. (d-f) Relative changes in capacitance for various strain rates of $\dot{\lambda} = 0.01\,\mathrm{s}^{-1}$, $0.1\,\mathrm{s}^{-1}$ and $1\,\mathrm{s}^{-1}$: (d) at a maximum strain of $10\,\%$ for 15, 50 and 100 cycles respectively; (e) at a maximum strain of $15\,\%$ for 15, 50 and 100 cycles respectively; (f) at a maximum strain of $20\,\%$ for 8, 50 and 200 cycles respectively.

the viscoelasticity of the Elastosil film. The sensor resets during unloading before the start of the next cycle. When the strain rate increases, the sensor does not have enough time to return completely to its original state. But after the load is removed, the sensor returns to its original state, as seen in the graphs after the completion of each cyclic test. In Figures 3 (d-f), for the constant strain value of 10%, 15% and 20%, as the strain rate increases, the range of capacitance change also increases. Thus, the viscoelastic properties of the elastomeric material are reflected in the behavior of the capacitance. This trend also continues for the stacked sensors. Considering one cycle of compression tests, the viscoelastic behavior of the elastomer is clearly visible at the strain rate $\dot{\lambda} = 1\,\mathrm{s}^{-1}$ for each sensor structure, cf. Figure 6 (c). At the low strain rate of $\dot{\lambda} = 0.01\,\mathrm{s}^{-1}$, the capacitance peak is clearly visible for each structure, but the unstacked sensor demonstrates stronger viscoelastic properties compared to stacked structures, cf. Figure 6 (a). Note that the capacitance change curve of unstacked sensor. At a strain rate of $\dot{\lambda} = 0.1\,\mathrm{s}^{-1}$, the peak begins to round off, cf. Figure 6 (b), and at a strain rate of $\dot{\lambda} = 1\,\mathrm{s}^{-1}$.

5.2 Stacked structure evaluation

If we compare the three structures of the tested sensors, then the structures 1x4ML-DES and 2x4ML-DES give basically the same results, but the resulting capacitance of the 2x4ML-DES is higher, cf. Figures 3, 4. In turn, the 3x4ML-DES structure has a more stable capacitance change, cf. Figures 5. In order to evaluate the stacked structures, we compare a maximum Gauge Factor (GF) of each structure for the strain rate of $\dot{\lambda} = 0.01\,\mathrm{s}^{-1}$ and at the strain value of 20%: $GF_{1x4ML-DES} = 0.67$, $GF_{2x4ML-DES} = 0.93$ and $GF_{3x4ML-DES} = 1.59$. Despite the lack of data for 2x4ML-DES at the strain of 10% and 15% , cf. Figure 4 (b, c), we used the MATLAB polyfit and polyval tools to predict GF values for these strains, cf. Figure 6 (d). The structure of 3x4ML-DES shows the highest GF and the most stable results compared to 1x4ML-DES and 2x4ML-DES structures. The higher stability of the stacked structure is probably due to the higher initial capacitance and the difference in the mechanical properties of the stacked and unstacked structures.

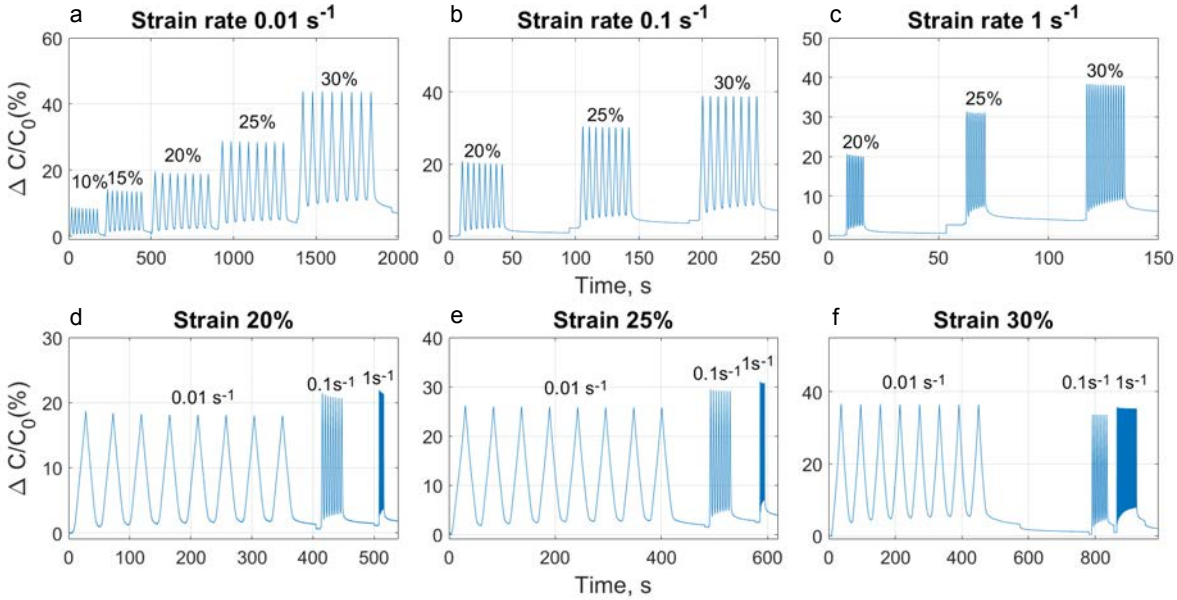

Figure 4: Cyclic compression tests on the 2x4ML-DES. (a-c) Relative changes in capacitance for various maximum strain values of 20%, 25% and 30%: (a) at a constant strain rate of $\dot{\lambda} = 0.01\,\mathrm{s}^{-1}$ with 8 cycles each; (b) at a constant strain rate of $\dot{\lambda} = 0.1\,\mathrm{s}^{-1}$ with 8 cycles each; (c) at a constant strain rate of $\dot{\lambda} = 1\,\mathrm{s}^{-1}$ for 8, 8 and 15 cycles respectively. (d-f) Relative changes in capacitance for various strain rates of $\dot{\lambda} = 0.01\,\mathrm{s}^{-1}$, $0.1\,\mathrm{s}^{-1}$ and $1\,\mathrm{s}^{-1}$: (d) at a maximum strain of $20\,\%$ with 8 cycles each; (e) at a maximum strain of $25\,\%$ with 8 cycles each; (f) at a maximum strain of $30\,\%$ for 8, 8, and 50 cycles respectively.

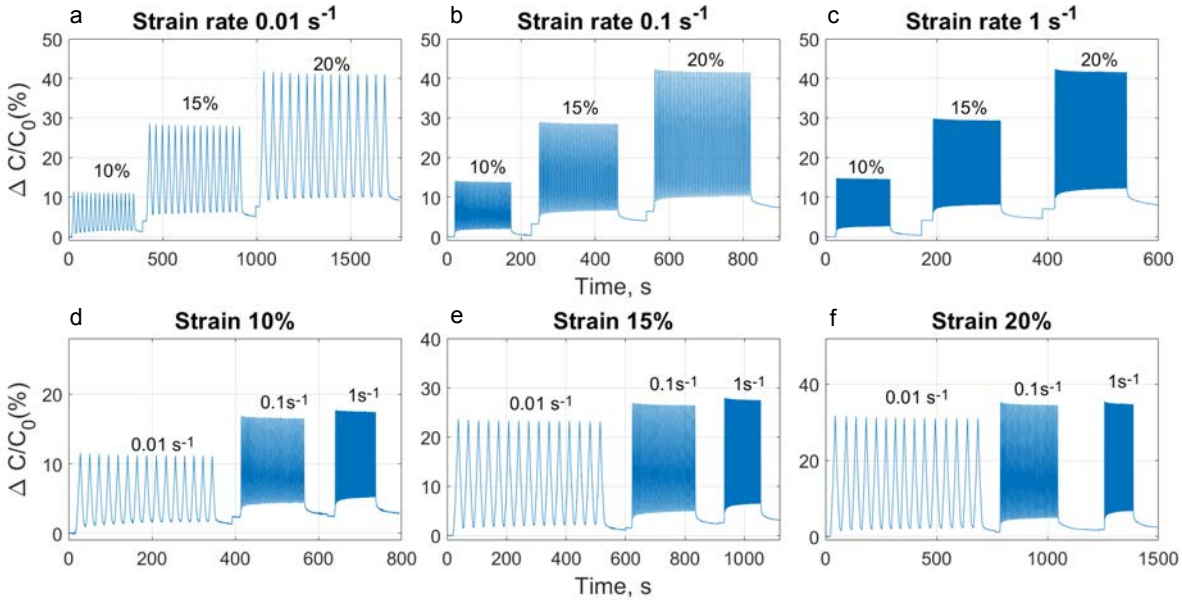

Figure 5: Cyclic compression tests on the 3x4ML-DES. (a-c) Relative changes in capacitance for various maximum strain values of 10%, 15% and 20%: (a) at a constant strain rate of $\dot{\lambda} = 0.01\,\mathrm{s}^{-1}$ with 15 cycles each; (b) at a constant strain rate of $\dot{\lambda} = 0.1\,\mathrm{s}^{-1}$ with 50 cycles each; (c) at a constant strain rate of $\dot{\lambda} = 1\,\mathrm{s}^{-1}$ with 100 cycles each. (d-f) Relative changes in capacitance for various strain rates of $\dot{\lambda} = 0.01\,\mathrm{s}^{-1}$, $0.1\,\mathrm{s}^{-1}$ and $1\,\mathrm{s}^{-1}$ for 15, 50 and 100 cycles respectively: (d) at a maximum strain of $10\,\%$; (e) at a maximum strain of $15\,\%$; (f) at a maximum strain of $20\,\%$.

6 CONCLUSIONS

In the current work, we described a stacking process of several multi-layer dielectric elastomer sensors. We have successfully manufactured and tested three types of sensor structure: one with four electrode layers (4ML-DES), another composed of two 4ML-DES stacked together

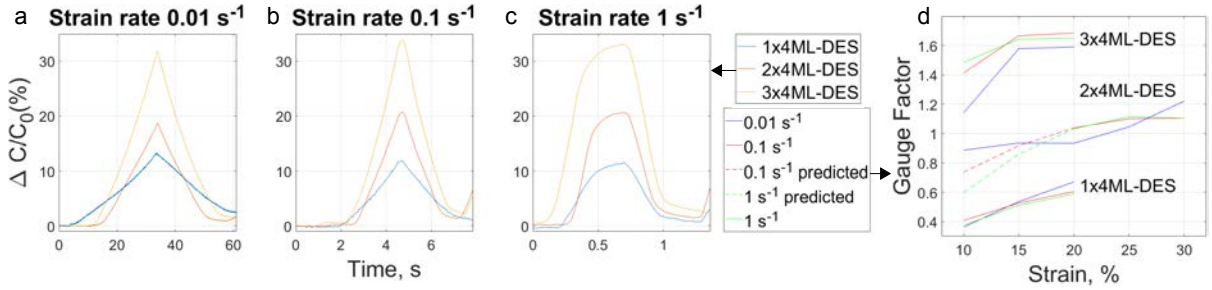

Figure 6: One cycle of compression tests for 1x4ML-DES, 2x4ML-DES and 3x4ML-DES. (a-c) at a maximum strain value of $20\,\%$. (a) for the strain rate of $\dot{\lambda} = 0.01\,\mathrm{s}^{-1}$, (b) $\dot{\lambda} = 0.1\,\mathrm{s}^{-1}$ and (c) $\dot{\lambda} = 1\,\mathrm{s}^{-1}$. (d) Dependence of GF on the maximum applied strain at various strain rates $\dot{\lambda} = 0.01\,\mathrm{s}^{-1}$, $0.1\,\mathrm{s}^{-1}$ and $1\,\mathrm{s}^{-1}$.

(2x4ML-DES), and a third consisting of three 4ML-DES stacked together (3x4ML-DES). The structure consisting of three sensors showed the most stable and predictable results. Thus, higher capacitance and high stability have been obtained for 3x4ML-DES structure. The influence of the viscoelasticity of the elastomeric material manifests itself in an increase in the lower threshold of capacitance change and a decrease in the upper threshold. In further studies, we will improve the manufacture process and investigate the production of a multi-layer structure without stacking.

Acknowledgement The support of the German Science Foundation (DFG) within the grants WA 2323/21-1, HE 7385/3-1, SCHL 1736/8-1 (project number: 466661922) and HE 7385/2-1 (418669083), and Europäischer Sozialfonds (ESF, European Social Fund) Plus and Freistaat Sachsen (Free State of Saxony) within the project: 100649621 is gratefully acknowledged.

REFERENCES

[1] Y. Jiang, S. Yin, J. Dong, and O. Kaynak, "A review on soft sensors for monitoring, control, and optimization of industrial processes," *IEEE Sensors Journal*, vol. 21, no. 11, pp. 12 868–12 881, 2021.

[2] J. Zhang, Q. Zhang, X. Liu, S. Xia, Y. Gao, and G. Gao, "Flexible and wearable strain sensors based on conductive hydrogels," *Journal of Polymer Science*, vol. 60, no. 18, pp. 2663–2678, 2022. [Online]. Available: https://onlinelibrary.wiley.com/doi/abs/10.1002/pol.20210935

[3] X. Cui, J. Guo, S. Araby, F. Abbassi, C. Zhang, A. L. Diaby, and Q. Meng, "Porous polyvinyl alcohol/graphene oxide composite film for strain sensing and energy-storage applications," *Nanotechnology*, vol. 33, no. 41, p. 415701, 2022.

[4] T. Q. Trung and N.-E. Lee, "Flexible and stretchable physical sensor integrated platforms for wearable human-activity monitoringand personal healthcare," *Advanced Materials*, vol. 28, no. 22, pp. 4338–4372, 2016. [Online]. Available: https://onlinelibrary.wiley.com/doi/abs/10.1002/adma.201504244

[5] S. Ma, J. Tang, T. Yan, and Z. Pan, "Performance of flexible strain sensors with different transition mechanisms: A review," *IEEE Sensors Journal*, vol. 22, no. 8, pp. 7475–7498, 2022.

[6] H. R. Na, H. J. Lee, J. H. Jeon, H.-J. Kim, S.-K. Jerng, S. B. Roy, S.-H. Chun, S. Lee, and Y. J. Yun, "Vertical graphene on flexible substrate, overcoming limits of crack-based resistive strain sensors," *npj Flexible Electronics*, vol. 6, no. 2, pp. 2397–4621, 2022.

[7] L. Cai, L. Song, P. Luan, Q. Zhang, N. Zhang, Q. Gao, D. Zhao, X. Zhang, M. Tu, F. Yang *et al.*, "Super-stretchable, transparent carbon nanotube-based capacitive strain sensors for human motion detection," *Scientific reports*, vol. 3, no. 1, pp. 1–9, 2013.

[8] A. Chhetry, S. Sharma, H. Yoon, S. Ko, and J. Y. Park, "Enhanced sensitivity of capacitive pressure and strain sensor based on $CaCu_3Ti_4O_{12}$ wrapped hybrid sponge for wearable applications," *Advanced Functional Materials*, vol. 30, no. 31, p. 1910020, 2020.

[9] F. Mo, Y. Huang, Q. Li, Z. Wang, R. Jiang, W. Gai, and C. Zhi, "A highly stable and durable capacitive strain sensor based on dynamically super-tough hydro/organo-gels," *Advanced Functional Materials*, vol. 31, no. 28, p. 2010830, 2021.

[10] X. Hu, F. Yang, M. Wu, Y. Sui, D. Guo, M. Li, Z. Kang, J. Sun, and J. Liu, "A super-stretchable and highly sensitive carbon nanotube capacitive strain sensor for wearable applications and soft robotics," *Advanced Materials Technologies*, vol. 7, no. 3, p. 2100769, 2022. [Online]. Available: https://onlinelibrary.wiley.com/doi/abs/10.1002/admt.202100769

[11] J. Guo, B. Zhou, R. Zong, L. Pan, X. Li, X. Yu, C. Yang, L. Kong, and Q. Dai, "Stretchable and highly sensitive optical strain sensors for human-activity monitoring and healthcare," *ACS Applied Materials & Interfaces*, vol. 11, no. 37, pp. 33 589–33 598, 2019, pMID: 31464425. [Online]. Available: https://doi.org/10.1021/acsami.9b09815

[12] R. Pelrine, R. Kornbluh, and G. Kofod, "High-strain actuator materials based on dielectric elastomers," *Advanced Materials*, vol. 12, pp. 1223 – 1225, 08 2000.

[13] A. Prokopchuk, A. Ewert, J. Menning, A. Richter, B. Schlecht, T. Wallmersperger, and E.-F. M. Henke, "Manufacturing of soft capacitive strain sensor based on dielectric elastomeric material for an elastic element of a jaw coupling," *submitted to Engineering Research Express*, 2023.

[14] F. Chen, K. Liu, Y. Wang, J. Zou, G. Gu, and X. Zhu, "Automatic design of soft dielectric elastomer actuators with optimal spatial electric fields," *IEEE Transactions on Robotics*, vol. 35, no. 5, pp. 1150–1165, 2019.

[15] A. Prokopchuk, A. Ewert, J. Menning, A. Richter, B. Schlecht, T. Wallmersperger, and E.-F. M. Henke, "Influence of manufacturing parameters on the quality of electrodes of a multi-layer capacitive strain sensor based on dielectric elastomers," *accepted in SPIE 2023+NDE*, 2023.